

AN IMPROVED STRAIN-ENERGY DENSITY MODEL CONSIDERING THE EFFECT OF MEAN STRESS

IZBOLJŠAN MODEL ZA NAPOVED GOSTOTE DEFORMACIJSKE ENERGIJE GLEDE NA VPLIV GLAVNE NAPETOSTI

Jing Li^{1*}, Yuan-ying Qiu¹, Xiao-long Tong², Lei Gao²

¹Xidian University, School of Mechatronic Engineering, No. 2 South Taibai Road, Xi'an 710071, PO Box 187, China

²AVIC Shenyang Aircraft Design & Research Institute, No. 40 Tawan Street, Shenyang, China

Prejem rokopisa – received: 2019-10-25; sprejem za objavo – accepted for publication: 2020-03-01

doi:10.17222/mit.2019.256

Based on the concept of strain-energy density, the Smith-Watson-Topper (SWT) parameter is corrected by introducing the mean stress-sensitivity factor to reflect the material's sensitivity to mean stress. In order to model the experimental data better, the mean stress-sensitivity factor is re-defined in three regimes in the Haigh diagram, which is different from the definition in the FKM Guideline. Procedures to determine the mean stress-sensitivity factor are also presented using the experimental data gained for two boundary states. Experimental verifications show that the modified criterion gives satisfactory results for all the six checked materials.

Keywords: mean stress, strain-energy density, mean stress-sensitivity factor, fatigue-life prediction

Na osnovi koncepta gostote deformacijske energije so avtorji Smith-Watson-Topperjev (SWT) parameter korigirali z uvedbo faktorja občutljivosti glavne napetosti. S tem so izrazili občutljivost materiala na glavno napetost. Zato, da bi bolje modelirali eksperimentalne podatke so avtorji redefinirali faktor občutljivosti glavne napetosti v treh področjih Haighovega diagrama, ki se razlikuje od definicije v navodilih oz. smernicah nemške organizacije FKM (nem.: Forschungskuratorium Maschinenbau). Avtorji prav tako v članku predstavljajo postopke za določitev faktorja občutljivosti glavne napetosti z uporabo eksperimentalnih podatkov, dobljenih pri dveh mejnih stanjih. Eksperimentalna potrditev modificiranih kriterijev je dala zadovoljive rezultate za vseh šest kontrolnih materialov.

Ključne besede: glavna napetost, gostota deformacijske energije, faktor občutljivosti glavne napetosti, napoved dobe trajanja

1 INTRODUCTION

As is known to all, fatigue failure is one of the most common types of failure and it must be taken into consideration when designing many structures and components. For this reason, over the years many researchers have focused on investigating and understanding the effect of variables that influence the fatigue life of many engineering components such as vehicles and aircraft, pressure vessels, gas turbines and so on. Engineering components in service usually experience non-symmetric cyclic loadings where mean stresses are present. Mean stresses significantly influence the fatigue lives of engineering components. Typically, the compressive mean stress is beneficial for fatigue life, which is longer than under a fully reversed uniaxial loading condition. Conversely, the tensile mean stress is detrimental to fatigue life, causing a reduction in useful life. For a design engineer, it is important to understand the effects of mean stress on the material fatigue behaviour. Therefore, many life-prediction models that account for the influence of the mean stress on fatigue life have been developed and verified in the last decades.¹⁻⁸

Early empirical models, developed by Gerber, Goodman, Haigh and Soderberg, were proposed to compensate for the tensile normal mean stress effects on the high-cycle fatigue strength.⁹ These empirical models can be plotted as constant life diagrams. The most useful graphical representations of the experimental-fatigue data are the constant life plots of the maximum stress, σ_{\max} , versus the minimal stress, σ_{\min} , or the stress amplitude, σ_a , versus the mean stress, σ_m . These constant life models can be experimentally determined from a family of Wöhler curves generated with specific values of σ_a and σ_m . Since 1960s, some fatigue test data has indicated that the tensile normal mean stress reduces the fatigue-strength coefficient, while the compressive normal mean stress increases it. Considered that the monotonic yield and ultimate tensile strengths are not appropriate for describing the fatigue behaviour of a material, Morrow¹⁰ suggested that the stress amplitude plus the mean stress could never exceed the fatigue-strength coefficient. Another popular method is the Smith-Watson-Topper (SWT) Equation (1),² in which the equivalent fully reversed stress amplitude, σ_{ar} , is expressed as follows:

$$\sigma_{ar} = \sqrt{\sigma_{\max} \sigma_a} \quad (1)$$

Considering the SWT equation, K. Walker¹ proposed a similar parameter by introducing an additional mate-

*Corresponding author's e-mail:
lijing02010303@163.com (Jing Li)

rial-dependent factor, w , in which the equivalent fully reversed stress amplitude, σ_{ar} , is given as:

$$\sigma_{ar} = \sigma_{max}^{1-w} \sigma_a^w \tag{2}$$

From Equations (1) and (2), it can be seen that the Walker relationship is equivalent to the SWT equation when the factor, w , equals 0.5. In other words, the SWT equation is a special case of the Walker equation. It should be noted that, mathematically, both SWT and Walker equations predict infinite life if $\sigma_{max} \leq 0$ and the fatigue crack can be considered not to start under this condition. A. Ince and G. Glinka⁵ reported that the estimations for the SWT model in the low-cycle fatigue regime were conservative, whereas the predictions for the Morrow model in the high-cycle fatigue regime were generally non-conservative. Based on these observations, A. Ince and G. Glinka⁵ made use of the SWT idea and modified the Morrow model in terms of the total equivalent strain amplitude. D. Kujawski¹¹ proposed a deviatoric version of the SWT parameter using the energy interpretation of the SWT parameter and its analogy with Neuber's rule. It was shown that the deviatoric SWT parameter provides a fairly good correlation for large compressive mean stresses.¹¹ Most recently, A. Ince and G. Glinka^{8,12} modified the SWT model on the basis of the concept of distortional strain energy to account for the mean-stress effects on fatigue life. In contrast to the Morrow and SWT models, the distortional strain energy-based SWT model provides better life predictions for high compressive mean stresses.

In the present paper, an improved strain-energy density model considering the effect of the mean stress is proposed by introducing the mean stress-sensitivity factor. In order to model the experimental data better, the mean stress-sensitivity factor is re-defined in three regimes in the Haigh diagram, which is different from the definition in the FKM Guideline. Besides, the procedures to determine the mean stress-sensitivity factor are also presented using the experimental data gained for two boundary states.

2 EXPERIMENTAL PART

2.1 Developed mean-stress correction model

From the perspective of the applied cyclic stresses, the fatigue damage of a component strongly correlates with the applied stress amplitude and the mean stress. The effect of the mean stress should be seriously considered in a fatigue analysis. In the high-cycle fatigue regime, the normal mean stresses have a significant effect on the fatigue behaviour of components. The initiation of microcracks accelerates the rate of crack propagation and the closing of microcracks retards the growth of cracks. In other words, the tensile mean normal stress is detrimental and compressive mean stress is beneficial in terms of fatigue strength. In the low-cycle

fatigue regime, the effect of the mean stress on the fatigue strength might be minimal since a larger plastic deformation significantly reduces any detrimental or beneficial effects.

N. E. Dowling et al.^{3,4} performed extensive comparisons of the tested data for steels, aluminium alloys and a kind of titanium alloy where the stress ratio, R , ranges from -2 to 0.45 . It was found that Goodman's model for life estimations is highly inaccurate, while Walker's model provides superior results if the additional mean-stress fitting parameter, w , is provided. Otherwise, both Morrow and SWT models give reasonable life predictions for steels. For aluminium alloys, the SWT model is recommended. N. E. Dowling et al.³⁻⁴ concluded that the SWT and Walker models provide relatively good results in most cases and are good choices for general use. However, we should remember that both the SWT and Walker models predict that a fatigue crack does not initiate if the maximum normal stress in the cycle is less than or equal to zero. This is in conflict with the observation that fatigue damage is observed under compression-compression loading.¹³ Besides, the material's sensitivity to the mean stress is not considered in the SWT model. To reflect different influences of the stress amplitude and mean stress on the fatigue damage, the mean stress-sensitivity-factor corrected-SWT parameter is developed on the basis of the strain energy density concept:

$$W_{MSWT} = \sigma_{ar} \varepsilon_a \tag{3}$$

Where ε_a and σ_{ar} denote the strain amplitude and the mean stress-sensitivity-factor-corrected effective stress amplitude, respectively.

The influence of mean stresses on fatigue damage described by the mean stress-sensitivity factor was introduced by Schütz,¹⁴ and it was included in the FKM Guideline.¹⁵ The mean stress-sensitivity factor is not a material constant, sensitive not only to the materials, but also to the loading levels.^{15,16} According to the FKM Guideline,¹⁵ the Haigh diagram based on a normal stress can be classified as four regimes as seen in **Figure 1**. It can be seen that Regimes I and IV have constant stress amplitudes over the mean stress range. This means that σ_{ar} is completely insensitive to the mean stress in these regimes. Regime II is characterized by L_{II} , which is the slope of the Haigh diagram in Regime II. In Regime III, the slope of the Haigh diagram is three times less sensitive to mean stresses. In classified regimes, the mean stress-sensitivity factor L_R can be written as follows:¹⁵

$$L_R = \begin{cases} 0 & \text{for } R \geq 0.5 \text{ or } R > 1 \\ L_{II} & \text{for } -\infty < R \leq 0 \\ L_{II/3} & \text{for } 0 < R < 0.5 \end{cases} \tag{4}$$

If we take the 7075-T651 aluminium alloy,¹³ for example, stress amplitude σ_a versus the tested fatigue life is plotted in **Figure 2** for uniaxial loadings with $R > 1$ and $R = -1$. If we take the 120-90-02 ductile cast iron¹⁷,

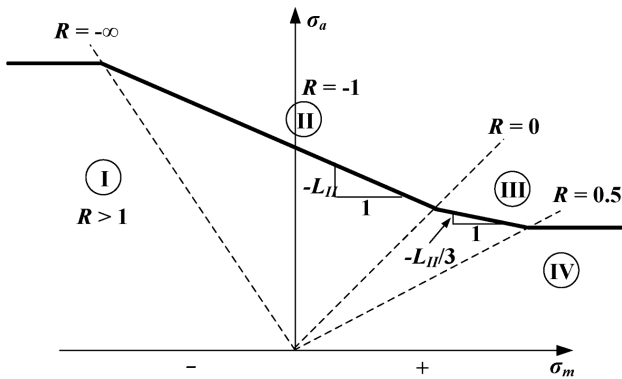


Figure 1: Mean stress-sensitivity factor in the Haigh diagram according to FKM Guideline¹⁵

for example, stress amplitude σ_a versus the tested fatigue life is plotted in Figure 3 for uniaxial loadings with $R = -1, 0.5$ and 0.75 . Unfortunately, both Figures 2 and 3 show that the mean stresses have substantial influences on the fatigue lives in Regimes I and IV, shown in Figure 1. Therefore, the mean stress-sensitivity factor defined by the FKM Guideline should be corrected in order to model the experimental data appropriately. Here, the mean stress-sensitivity factor L_R is redefined with the following equation to model the experimental data on the basis of the corrected SWT parameter:

$$L_R = \begin{cases} 0.75L_{II} & \text{for } -\infty \leq R < -1 \text{ or } R > 1 \\ L_{II} & \text{for } -1 < R \leq 0.5 \\ L_{II/3} & \text{for } 0.5 < R < 1 \end{cases} \quad (5)$$

In this equation, L_{II} is the mean stress-sensitivity factor for fatigue loadings with stress ratio R ranging from -0.1 to 0.5 . The key solution for the proposed parameter is the use of the tested data to obtain the mean stress-sensitivity factor. According to this definition, the Haigh diagram based on a normal stress can be classified as three regimes, as shown in Figure 4. It can be seen that factor L_R can be determined as long as the mean stress-sensitivity factor L_{II} , shown in Figure 4, is ob-

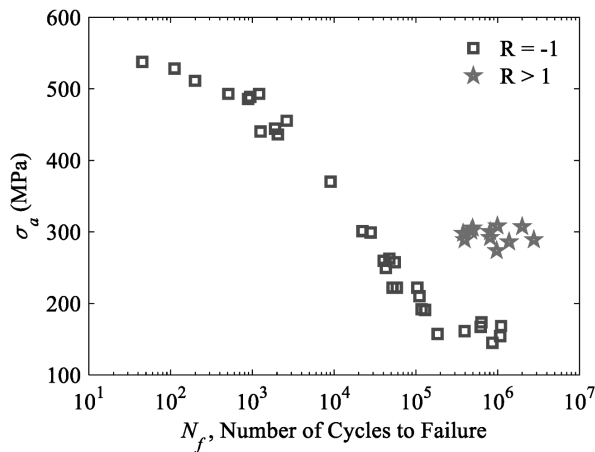


Figure 2: Stress life under uniaxial fatigue loadings with $R = -1$ and $R > 1$ for 7075-T651

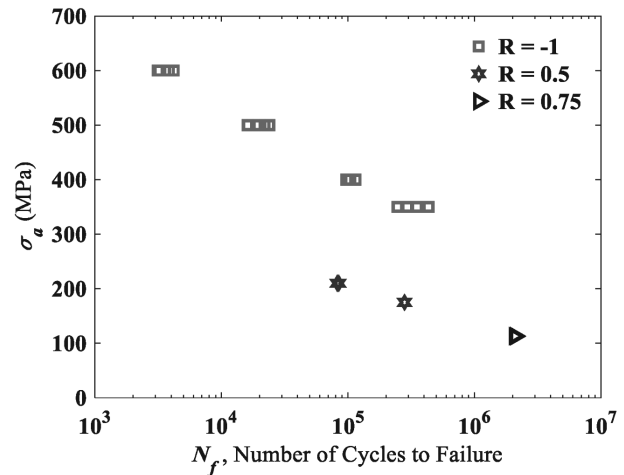


Figure 3: Stress life under uniaxial fatigue loadings with $R = -1, 0.5$ and 0.75 for 120-90-02 ductile cast iron

tained. Then, the corrected effective stress amplitude σ_{ar} in the classified regimes can be written as follows:

$$\sigma_{ar} = \begin{cases} \sigma_a + 0.75L_{II}\sigma_m & \text{for } -\infty \leq R < -1 \text{ or } R > 1 \\ \sigma_a + L_{II}\sigma_m & \text{for } -1 < R \leq 0.5 \\ \frac{1+3L_{II}}{1+L_{II}}(\sigma_a + \frac{L_{II}}{3}\sigma_m) & \text{for } 0.5 < R < 1 \end{cases} \quad (6)$$

The key procedure in the determination of the mean stress-sensitivity factor, L_{II} , in Regime II, is the use of the experimental data gained for two boundary states, i.e., the tension-compression with a stress ratio of $R = -1$ and another one with a significant mean stress value such as popular unilateral tensile ratio of $R = 0$. The value of the mean stress-sensitivity factor, L_{II} , can be determined from the aforementioned test data as the value, which minimizes the sum (P) of the squared differences between $\sigma_a \varepsilon_a$ obtained from the tension-compression data and $(\sigma_a + L_{II} \sigma_m) \varepsilon_a$ calculated from the test data with the mean stress. P is defined in Equation (7) and Figure 5 illustrates how to compute P .

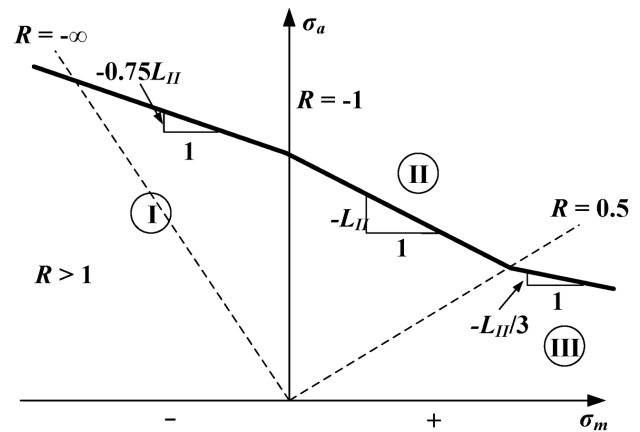


Figure 4: Mean stress-sensitivity factor in the Haigh diagram according to the developed method

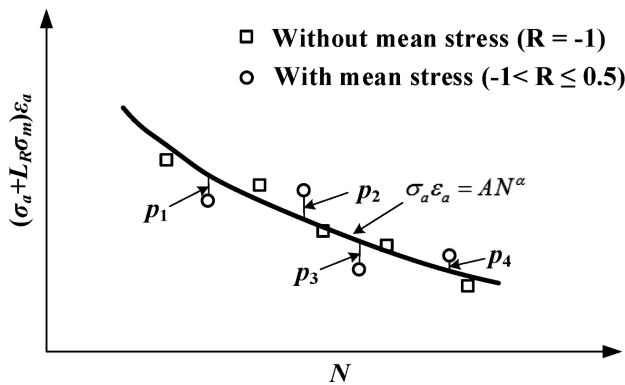


Figure 5: Schematic illustration of the sum (P) of the squared differences between $\sigma_a \epsilon_a$ predicted using the fatigue loading with $R = -1$ and $(\sigma_a + L_{II} \sigma_m) \epsilon_a$

$$P = \sum_{i=1}^n p_i^2 = \sum_{i=1}^n \left\{ AN_i^\alpha - (\sigma_{a,i} + L_{II} \sigma_{m,i}) \epsilon_{a,i} \right\}^2 \quad (7)$$

Here, n is the number of the mean-stress test points. For the constants A and α , a curve may be estimated with the least-squares method based on the tested data of fully reversed uniaxial loading in the form of $\sigma_a \epsilon_a = AN^\alpha$.

It is necessary to point out here that the factor L_{II} determined using the aforementioned procedure is totally different from the one determined by the FKM Guideline. In the proposed procedure, the influences of strain terms on the fatigue life are also considered to determine the mean stress-sensitivity factor, L_{II} , in Regime II of **Figure 4**. In contrast to the proposed method, only the stress terms are considered in the FKM Guideline. Therefore, the mean stress-sensitivity factor determined on the basis of the FKM Guideline cannot be applied in the proposed model.

3 EVALUATION OF THE DEVELOPED MEAN-STRESS CORRECTION MODEL

Fatigue experimental data for six kinds of material available in the literature^{13, 17-20} were used to assess the capability of the modified model, which takes into account the influence of mean stress. While choosing the appropriate data sets, particular attention should be focused on their completeness so that the considered materials include:

- Wöhler curve for alternating stress ($R = -1$);
- Wöhler curve obtained with a significant mean-stress value used for the determination of the factor L_{II} ; and
- experimental data for different stress ratios of mean stresses. From the data sets available in the literature, specific fatigue experimental results were considered to perform the verifications.

The materials included the 7075-T651 aluminium alloy,¹³ 120-90-02 ductile cast iron,¹⁷ SAE 1045 steel,¹⁸ Ti-6Al-4V ELI titanium alloy¹⁹, LC4 and LC9 aluminium alloys.²⁰ The constants A and α of these materials are listed in **Table 1**; they were determined by fitting the

experimental data of the materials with $R = -1$. **Figures 6 to 11** present the fatigue-life correlations based on the proposed parameter for the six kinds of material subjected to different mean-stress levels, for which both tensile and compressive mean stresses were considered.

Table 1: Constants of the considered materials fitted from the experimental data with $R = -1$

Materials	7075-T651	Cast iron	SAE 1045	Ti-6Al-4V ELI	LC4	LC9
A	37.3	34.9	67.8	30.7	382.7	188.9
α	-0.3516	-0.3132	-0.2374	-0.1855	-0.6017	-0.5266

3.1 7075-T651 aluminium alloy

We used the fatigue test results and material properties of the 7075-T651 aluminium alloy obtained by T. Zhao and Y. Jiang¹³ to verify the proposed model. Strain-controlled, fully reversed uniaxial loading as well as uniaxial loadings with both compressive and tensile mean stresses were performed on solid specimens. The mean stress-sensitivity factor, L_{II} , was determined with the aforementioned procedure using the uniaxial loadings with $R = -1$ and 0. It is found that $L_{II} = 1.0$ can correlate with the experimental data well. The fatigue-life correlations based on the parameter proposed for the 7075-T651 aluminium alloy are plotted in **Figure 6**. A good fatigue-life correlation is obtained for this material within a factor of 3.

3.2 120-90-02 ductile cast iron

120-90-02 ductile cast iron components were tested by N. M. Meyer¹⁷ under various mean stress levels with $R = -7, -3, -1, 0, 0.33, 0.5$ and 0.75 . Based on the uniaxial test data with $R = -1$ and 0, a least squares fit using the aforementioned procedure resulted in $L_{II} = 1.0$. **Figure 7** shows the fatigue-life correlations based on the parameter proposed for 120-90-02 ductile cast iron. The

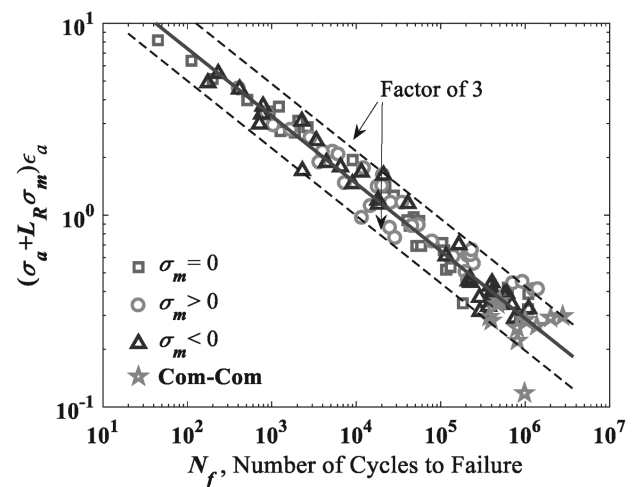


Figure 6: Comparison of experimental mean stress fatigue data for 7075-T651 aluminum alloy¹³

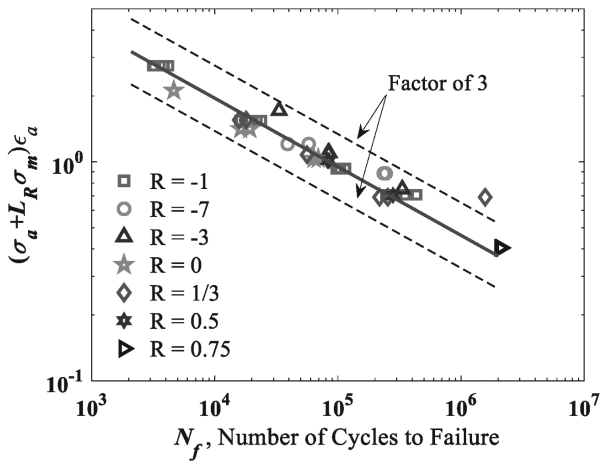


Figure 7: Comparison of experimental mean stress fatigue data for 120-90-02 ductile cast iron¹⁷

fatigue-life correlation for this material fell within a factor of 3.

3.3 SAE 1045 steel

Uniaxial-fatigue experiments with strain ratios $R = -2, -1, 0$ and 0.5 were conducted on SAE 1045 steel in ambient air.¹⁸ The stress amplitude and mean stress applied in the proposed model are midlife values, listed in reference.¹⁸ A least squares fit of the data with $R = -1$ and 0 resulted in $L_{II} = 1.0$. A log-log plot of the experimental lives under various loadings versus the proposed parameter is shown in **Figure 8**. This figure illustrates how successfully the proposed parameter can correlate with the experimental data, being within a factor of 3 under the considered loading conditions.

3.4 Ti-6Al-4V ELI titanium alloy

E. Carrion et al.¹⁹ performed fatigue tests on Ti-6Al-4V ELI titanium alloy components under various

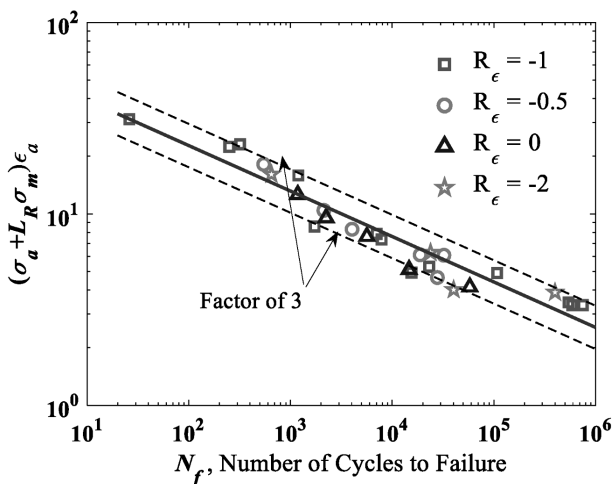


Figure 8: Comparison of experimental mean stress fatigue data for SAE 1045 steel¹⁸

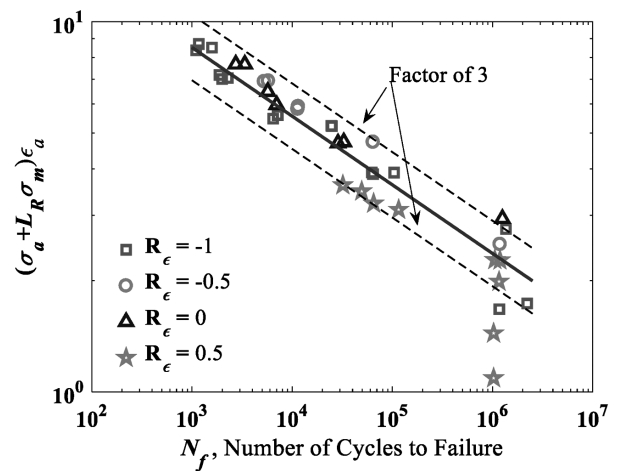


Figure 9: Comparison of experimental mean stress fatigue data for Ti-6Al-4V ELI titanium alloy¹⁹

mean-strain levels with strain ratios $R_ε = -1, -0.5, 0$ and 0.5 . The mean stresses for different mean strain conditions were also presented in ¹⁹. The least squares fit of the experimental data with $R_ε = -1$ and 0 resulted in $L_{II} = 0.78$. The fatigue-life correlations based on the parameter proposed for this material are plotted in **Figure 9**. It can be seen from this figure that the fatigue-life correlation falls within a factor of 3.

3.5 LC4 aluminium alloy

Uniaxial-fatigue experiments with mean stresses $\sigma_m = 0, 68.6, 137.2$ and 205.8 MPa were conducted on an LC4 aluminium alloy to experimentally investigate the fatigue behaviour.²⁰ Using the aforementioned procedure, the experimental data with $\sigma_m = 0$ and 137.2 MPa come to fit into one curve, resulting in $L_{II} = 0.51$. A log-log plot of the experimental lives under various mean-stress levels versus the proposed parameter is shown in **Figure 10**. It is shown that most of the predictions for this material are within a factor of 3.

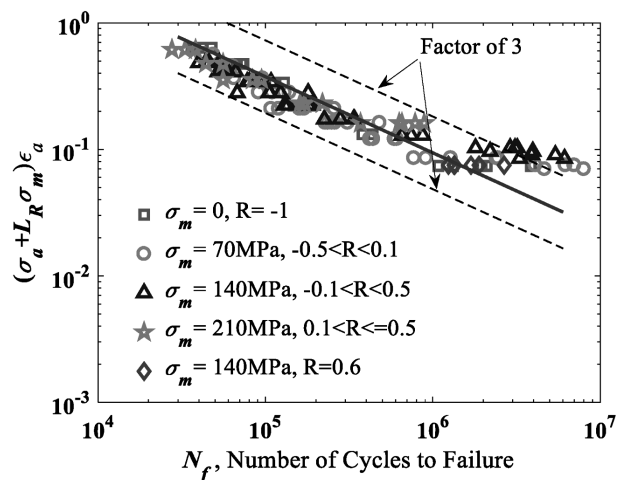


Figure 10: Comparison of experimental mean stress fatigue data for LC4 aluminium alloy²⁰

3.6 LC9 aluminium alloy

The fatigue test results and material properties of the LC9 aluminium alloy were also taken from reference²⁰. Stress-controlled uniaxial loadings with $R = -1, 0.1$ and 0.5 were performed on solid specimens. Based on the aforementioned procedure, a least squares fit using the uniaxial test data with $R = -1$ and 0.1 resulted in $L_{II} = 1.0$. **Figure 11** shows the fatigue-life correlations based on the parameter proposed for this material. A good fatigue-life correlation is obtained for the LC9 aluminium alloy within a factor of 3.

Based on the strain-energy density concept, the SWT model can be rewritten as²:

$$W_{SWT} = \sigma_{\max} \epsilon_a = AN^\alpha \tag{8}$$

At a given life, $\sigma_a \epsilon_a$ for a fully reversed test is equal to $\sigma_{\max} \epsilon_a$ for a mean-stress test. It is easy to derive that the proposed model reduces to the SWT model under the fully reversed uniaxial loading. Therefore, the SWT model was checked only by using and comparing the experimental data of the aforementioned six materials tested under uniaxial loadings with mean stress. Experimental verifications of the SWT model and the proposed one are plotted in **Figures 12** and **13**, respectively. **Figure 12** shows that, except for the LC4 aluminium alloy, the SWT model presents relatively satisfactory predictions for uniaxial loading with $\sigma_m > 0$. However, non-conservative predictions are obtained for the considered materials tested under uniaxial loading with $\sigma_m < 0$. In contrast to the SWT model, **Figure 13** shows that the proposed model can give satisfactory predictions for all the six considered materials whether the mean stress is positive or negative.

In order to evaluate the capability of the life-prediction models more clearly, the evaluation based on the error criterion, $E(s)$, is given as²¹:

$$E(s) = \frac{NDF}{NTD} \tag{9}$$

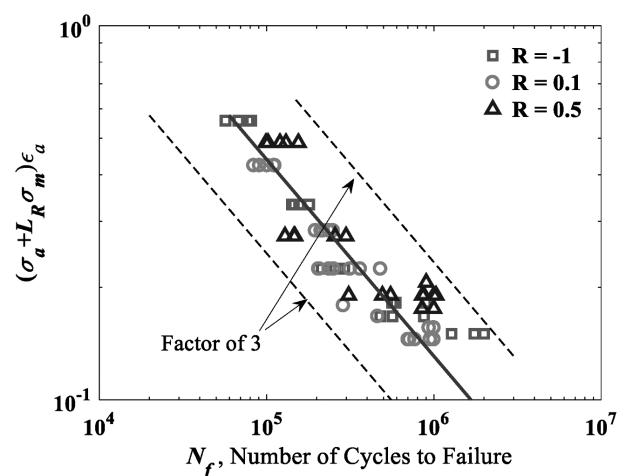


Figure 11: Comparison of experimental mean stress fatigue data for LC9 aluminium alloy²⁰

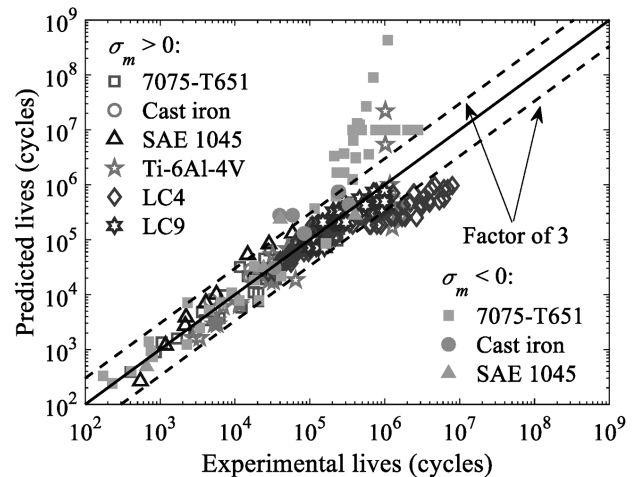


Figure 12: Prediction of fatigue lives by SWT model under uniaxial loadings with mean stress^{13,17-20}

where NDF is number of data falling within $1/s \leq N_p/N_t \leq s$, NTD is number of total data and N_p, N_t are the predicted and tested lives, respectively. It can be seen from Equation (9) that the closer the $E(s)$ is to unity, the better is the prediction.

Table 2 summarizes all the checked models' predicted ranges for different materials and mean-stress levels. Considering all the data with $\sigma_m > 0$ in **Figures 12** and **13**, 83.6 % and 91.8 % of the data, respectively, predicted by the SWT model and the proposed one fall within a scatter band of 3. However, considering all the data with $\sigma_m < 0$, only 43.1 % of the data predicted by the SWT model fall within the scatter band of 3. In contrast to the SWT model, over 96.6 % of the same tested data predicted by the proposed model fall within the scatter band of 3. Therefore, the proposed model appears to be relatively accurate and promising, although additional data need to be further verified for its robustness.

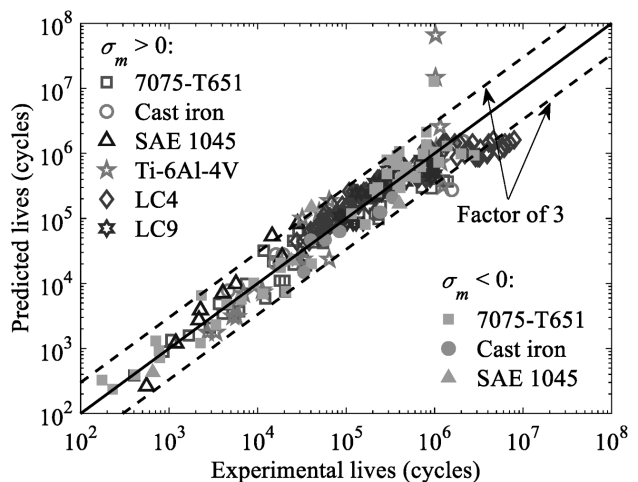


Figure 13: Prediction of fatigue lives by the proposed model under uniaxial loadings with mean stress^{13,17-20}

Table 2: Comparison of SWT the MSWT models using the error criterion

	$\sigma_m > 0$			$\sigma_m < 0$		
	$E(2)$	$E(3)$	$E(5)$	$E(2)$	$E(3)$	$E(5)$
SWT	73.7%	83.6%	91.4%	39.7%	43.1%	56.9%
MSWT	80.2%	91.8%	97.8%	75.9%	96.6%	98.3%

4 CONCLUSIONS

1. An improved strain-energy density model considering the effect of mean stress is proposed, i.e.,

$$W_{MSWT} = \sigma_{ar} \varepsilon_a$$

with

$$\sigma_{ar} = \begin{cases} \sigma_a + 0.75L_{II}\sigma_m & \text{for } -\infty \leq R < -1 \text{ or } R > 1 \\ \sigma_a + L_{II}\sigma_m & \text{for } -1 < R \leq 0.5 \\ \frac{1+3L_{II}}{1+L_{II}}(\sigma_a + \frac{L_{II}}{3}\sigma_m) & \text{for } 0.5 < R < 1 \end{cases}$$

2. Based on the least-squares method, the value of the mean stress-sensitivity factor, L_{II} , in the proposed method can be determined from two boundary states: the tension-compression with the stress ratio $R = -1$ and another one with a significant mean-stress value such as popular unilateral tensile $R = 0$.
3. The factor L_{II} determined using the FKM Guideline cannot be applied in the proposed method.

Acknowledgment

The authors gratefully acknowledge the financial support of the National Natural Science Foundation of China (No. 51601221), the Natural Science Basic Research Plan in the Shaanxi Province of China (No. 2019JQ-353) and the Fundamental Research Funds for the Central Universities (No. JB180402).

5 REFERENCES

¹ K. Walker, The effect of stress ratio during crack propagation and fatigue for 2024-T3 and 7075-T6 aluminium, ASTM STP 462, Am. Soc. for Testing and Materials, West Conshohocken, PA, 1970, 1–14
² K. N. Smith, P. Watson, T. H. Topper, A Stress strain function for the fatigue of materials, *J. Mater.*, 5 (1970), 767–778
³ N. E. Dowling, Mean stress effects in strain life fatigue, *Fatigue Fract. Eng. Mater. Struct.*, 32 (2009), 1004–1019, doi:10.1111/j.1460-2695.2009.01404.x

⁴ N. E. Dowling, C. A. Calhoun, A. Arcari, Mean stress effects in stress life fatigue and the Walker equation, *Fatigue Fract. Eng. Mater. Struct.*, 32 (2009), 163–179, doi:10.1111/j.1460-2695.2008.01322.x
⁵ A. Ince, G. Glinka, A modification of Morrow and Smith-Watson-Topper mean stress correction models, *Fatigue Fract. Eng. Mater. Struct.*, 34 (2011), 854–867, doi:10.1111/j.1460-2695.2011.01577.x
⁶ R. Burger, Y. Lee, Assessment of the mean stress sensitivity factor method in stress life fatigue predictions, *J. Test. Eval.*, 41 (2013), 200–206, doi:10.1520/JTE20120035
⁷ S. P. Zhu, Q. Lei, H. Z. Huang, Y. J. Yang, W. W. Peng, Mean stress effect correction in strain energy-based fatigue life prediction of metals, *Int. J. Damage Mech.*, 26 (2017), 1219–1241, doi:10.1177/1056789516651920
⁸ A. Ince, A generalized mean stress correction model based on distortional strain energy, *Int. J. Fatigue*, 104 (2017), 273–282, doi:10.1016/j.ijfatigue.2017.07.023
⁹ G. P. Sendeckyi, Constant life diagrams – a historical review, *Int. J. Fatigue*, 23 (2001), 347–353, doi:10.1016/S0142-1123(00)00077-3
¹⁰ J. Morrow, *Fatigue design handbook*, Society of Automotive Engineers, Warrendale, PA, 1968, 21–29
¹¹ D. Kujawski, A deviatoric version of the SWT parameter, *Int. J. Fatigue*, 67 (2014), 95–102, doi:10.1016/j.ijfatigue.2013.12.002
¹² A. Ince, A mean stress correction model for tensile and compressive mean stress fatigue loadings, *Fatigue Fract. Eng. Mater. Struct.*, 40 (2017), 939–948, doi:10.1111/ffe.12553
¹³ T. Zhao, Y. Jiang, Fatigue of 7075-T651 aluminium alloy, *Int. J. Fatigue*, 30 (2008), 834–849, doi:10.1016/j.ijfatigue.2007.07.005
¹⁴ W. Schütz, Über eine Beziehung zwischen der Lebensdauer bei konstanter und veränderlichen Beanspruchungs Amplituden und ihre Anwendbarkeit auf die Bemessung von Flugzeugbauteilen, *Zeitschrift für Flugwissenschaften*, 15 (1967), 407–419
¹⁵ S. A. Mckelvey, Y. L. Lee, M. E. Barkey, Stress-based uniaxial fatigue analysis using methods described in FKM-guideline, *J. Fail. Anal. and Preven.*, 12 (2012), 445–484, doi:10.1007/s11668-012-9599-4
¹⁶ Y. L. Lee, J. Pan, R. Hathaway, M. E. Barkey, *Fatigue testing and analysis: theory and practice*, Elsevier, Oxford, UK, 2005, 243
¹⁷ N. M. Meyer, Effects of mean stress and stress concentration on fatigue behavior of ductile iron, MSc Thesis in Mechanical Engineering, the University of Toledo, 2014
¹⁸ T. Wehner, A. Fatemi, Effects of mean stress on fatigue behaviour of a hardened carbon steel, *Int. J. Fatigue*, 13 (1991), 241–248
¹⁹ P. E. Carrion, N. Shamsaei, S. R. Daniewicz, R. D. Moser, Fatigue behavior of Ti-6Al-4V ELI including mean stress effects, *Int. J. Fatigue*, 99 (2017), 87–100, doi:10.1016/j.ijfatigue.2017.02.013
²⁰ Z. T. Gao, *A handbook on fatigue properties of aeronautical materials*, Beijing Material Research Institute, Beijing, 1981, 87 (in Chinese)
²¹ J. Li, Z. P. Zhang, Q. Sun, C. W. Li, Multiaxial fatigue life prediction for various metallic materials based on the critical plane approach, *Int. J. Fatigue*, 33 (2011), 90–101, doi:10.1016/j.ijfatigue.2010.07.003